Brain Structure and Function (2019) 224:1051–1066
https://doi.org/10.1007/s00429-018-01822-4

ORIGINAL ARTICLE

Sledge runner fasciculus: anatomic architecture and tractographic morphology

Christos Koutsarnakis[1,2,3,7] · Aristotelis. V. Kalyvas[1,3,7] · Georgios P. Skandalakis[1,6] · Efstratios Karavasilis[4] · Foteini Christidi[4,5] · Spyridon Komaitis[1,3,7] · George Velonakis[4] · Faidon Liakos[1] · John Emelifeonwu[1,2] · Zoi Giavri[8] · Theodosis Kalamatianos[7] · Nikolaos Kelekis[4] · George Stranjalis[1,3,7]

Received: 16 March 2018 / Accepted: 19 December 2018 / Published online: 3 January 2019

Abstract

The sledge runner fasciculus (SRF) has been recently identified as a discrete fiber tract of the occipital lobe and has been allegedly implicated in the axonal connectivity of cortical areas conveying spatial navigation and visuospatial imagery. However, detailed knowledge regarding its anatomic and tractographic morphology is lacking. We thus opted to investigate the anatomy and connectivity of the SRF through cadaveric dissections and DTI studies. Twenty normal, adult, cerebral, cadaveric hemispheres treated with the Klingler's method were dissected through the fiber microdissection technique and 35 healthy participants from the MGH-USC Adult Diffusion Dataset (Human Connectome available dataset) underwent a tailored DTI protocol aiming to investigate the structural architecture of the SRF. SR was identified as a discrete fiber pathway, just under the U fibers of the medial occipital lobe, exhibiting a dorsomedial–ventrolateral trajectory and connecting the cortical areas of the anterior cuneus, anterior lingula, isthmus of the cingulum and posterior parahippocampal gyrus. The topography of the SR in relation to adjacent fiber pathways such as the cingulum, major forceps and stratum calcarinum is clearly delineated. Dissection and tractographic findings showed a good correspondence regarding SR topography, morphology and axonal connectivity. Our results support the hypothesis that the SRF is involved in the structural axonal connectivity of cerebral areas that strongly activate during spatial navigation and visuospatial imagery. Furthermore detailed anatomo-imaging evidence is provided on the microanatomic architecture of this newly discovered fiber tract.

Keywords Sledge runner · Brain connectivity · White matter anatomy · Occipital lobe · Visuospatial imagery · Spatial navigation

Christos Koutsarnakis and Aristotelis. V. Kalyvas contributed equally to this study.

✉ Christos Koutsarnakis
ckouts@hotmail.co.uk

1 Athens Microneurosurgery Laboratory, Evangelismos Hospital, Athens, Greece

2 Edinburgh Microneurosurgery Education Laboratory, Department of Clinical Neurosciences, Western General Hospital, Edinburgh, UK

3 Department of Neurosurgery, Evangelismos Hospital, National and Kapodistrian University of Athens, Athens, Greece

4 2nd Department of Radiology, Medical School, General University Hospital "Attikon", National and Kapodistrian University of Athens, Athens, Greece

5 1st Department of Neurology, Medical School, Aeginition Hospital, National and Kapodistrian University of Athens, Athens, Greece

6 Medical School, National and Kapodistrian University of Athens, Athens, Greece

7 Hellenic Center for Neurosurgical Research, "Petros Kokkalis", Athens, Greece

8 Department of Electrical and Computer Engineering, National Technical University of Athens, Athens, Greece

Introduction

The recent revival of the white matter fiber dissection technique—first described by Klingler—and its incorporation not only to neuroanatomical education but also to neurocognitive research, in combination with the advent of sophisticated neuroimaging methods such as functional magnetic resonance imaging (fMRI) and diffusion tensor imaging (DTI) have led to a more profound understanding of the brain connectivity and anatomo-functional organization (Catani et al. 2002; Fernandez-Miranda et al. 2008a, b; Klingler 1935; Klingler and Ludwig 1956; Mamata et al. 2002; Mandonnet et al. 2006; Mori et al. 1999; Ture et al. 2000; Peltier et al. 2010a; Duffau et al. 2002, 2005; Arnts et al. 2014; Koutsarnakis et al. 2015). The coining of the modern concept of brain hodotopy (deriving from the Greek words hodos meaning road, pathway and topos meaning place) moves away from the classical localizationist view and introduces a new model of perceiving cerebral function not only as a cortical phenomenon but as an integral cortico-subcortical epiphenomenon (Duffau 2006, 2011, 2015, 2017; Duffau et al. 2014; Catani and de Schotten 2012; Catani et al. 2003, 2005; De Benedictis and Duffau 2011). In other words, apart from an intact cortical organization, the integrity of the white matter axonal connectivity is essential to cerebral physiology and function.

Since brain anatomy and function are tightly and reciprocally connected, a special interest has aroused over the past few years regarding the intricate morphology and architecture of white matter pathways previously described in core neuroanatomical texts, aiming not only to refine anatomical knowledge but mainly to improve our understanding of cerebral connectivity and function (Fernandez-Miranda et al. 2008b; Peltier et al. 2010a, b; Martino et al. 2010; Pascalau et al. 2018; Koutsarnakis et al. 2016). Recent literature has thus revisited the subcortical anatomy of various, eloquent and non-eloquent fiber tracts using white matter dissections and DTI techniques with the overarching goal to combine the extracted evidence with functional data, thus providing a refined concept of brain organization (Catani et al. 2002, 2005; Fernandez-Miranda et al. 2008a, b; Koutsarnakis et al. 2015, 2016, 2017b, 2018; Mamata et al. 2002; Mandonnet et al. 2006; Mori et al. 1999; Ture et al. 2000; Peltier et al. 2010a, b; Duffau et al. 2002, 2005, 2014; Duffau 2006, 2015; Catani and de Schotten 2012; Martino et al. 2010; Kier et al. 2004a, b).

In this regard, we opted to investigate, through cadaveric fiber microdissections and an vivo DTI study, the structural architecture of a recently identified fiber tract known as the "sledge runner fasciculus" (Gungor et al. 2017; Vergani et al. 2014; Baydin et al. 2017; Beyh et al. 2017). This white matter pathway has been allegedly implicated in the axonal connectivity of high level cortical areas, such as the parahippocampal place area (PPA) and posterior cingulate or retrosplenial cortex (PCC-RSC), which represent key hubs of the neural circuit underlying the cognitive ability of spatial navigation and visuospatial imagery (Whittingstall et al. 2014; Epstein et al. 2017, 2007a, b; Epstein 2008; Ino et al. 2002; Epstein and Kanwisher 1998; Spiers and Maguire 2006, 2007; Aguirre and D'Esposito 1999; O'Craven and Kanwisher 2000; Maguire et al. 1997; Beyh et al. 2017). Indeed, meticulous neuropsychological assessment of patients harbouring posterior circulation infarcts with posterior parahippocampal and/or retrosplenial area damage indicates increasing difficulty or even inability of these individuals to identify large scale scenes, such as landscapes or cityscapes, and further inability of proper self-navigation and way finding in familiar environments (Aguirre and D'Esposito 1999; Barrash et al. 2000; Pallis 1955; Hecaen et al. 1980; Takahashi et al. 1997; Ino et al. 2007; Katayama et al. 1999; Bottini et al. 1990; Osawa et al. 2008; Ploner et al. 2000).

In this study, we provide anatomic and imaging data on the topography, morphology and axonal connectivity of the sledge runner fasciculus (SRF) using the Klinger's dissection technique and DTI tractography on the publicly available dataset from the Human Connectome Project. Our overarching goal is to clarify the intricate subcortical architecture of this recently identified white matter tract believed to subserve spatial navigation and visuospatial imagery.

Materials and methods

The study was divided in two parts, including cadaveric microanatomic white matter fiber dissections and a DTI imaging protocol in normal individuals.

White matter fiber micro-dissection

Twenty normal, adult, cadaveric cerebral hemispheres (11 right hemispheres—9 left hemispheres) obtained from 20 different cadavers previously fixed in a 10–15% formalin solution for a minimum period of 8 weeks, were investigated. Following careful removal of the arachnoid membrane and vessels, all specimens underwent the Klingler's procedure (freeze–thaw process) and were subsequently investigated using the fiber dissection technique and the microscope (Carl Zeiss OPMIR Plus, Carl Zeiss AG, Oberkochen, Germany) (Klingler 1935; Klingler and Ludwig 1956; Ture et al. 2000; Koutsarnakis et al. 2015).

Given that the sledge runner fasciculus lies in the depth of the medial and medio-basal occipital lobe (Gungor et al. 2017; Vergani et al. 2014; Baydin et al. 2017), we opted to perform regional (confined to the occipital lobe),

microanatomic dissections in a medial to lateral direction in all 20 hemispheres.

The regional sulcal anatomy consisting of the parieto-occipital sulcus (demarcating the precuneus and isthmus of the cingulate gyrus from the cuneus), calcarine fissure (demarcating the cuneus from the lingual gyrus) and their common stem (demarcating the lingual and posterior parahippocampal gyri from the isthmus of the cingulate gyrus) the collateral sulcus (demarcating the parahippocampal from the fusiform gyrus) and sub-parietal sulcus (demarcating the isthmus of the cingulate gyrus from the precuneus) were readily identified in all specimens (Fig. 1). The fiber microdissections were initially focused on the area of the cuneus and lingual gyrus and were further extended to the adjacent cerebral region of the cingulate isthmus, posterior half of the precuneus and posterior part of the parahippocampal gyrus with the aim to study and record the morphology, topography and dimensions of the sledge runner fasciculus (Fig. 2). Special emphasis was also placed on the correlative anatomy of the sledge runner fasciculus with the sulci gyri, adjacent white matter pathways and ventricular compartments.

The dissection tools used consisted of fine metallic periosteal elevators, various sized anatomical forceps, and micro-scissors (Koutsarnakis et al. 2015, 2016). Numerous photographs were obtained during cadaveric dissections to illustrate the regional cortical and subcortical anatomy of interest. Of note is that the dissection photos included in this study have not been edited by picture enhancing software so that they closely resemble the anatomy encountered during standard fiber micro-dissections in the setting of a microneurosurgery laboratory (Koutsarnakis et al. 2015, 2016, 2017a).

DTI imaging

Data used in the preparation of this work were obtained from the Human Connectome Project (HCP) database (https://ida.loni.usc.edu/login.jsp). The HCP project

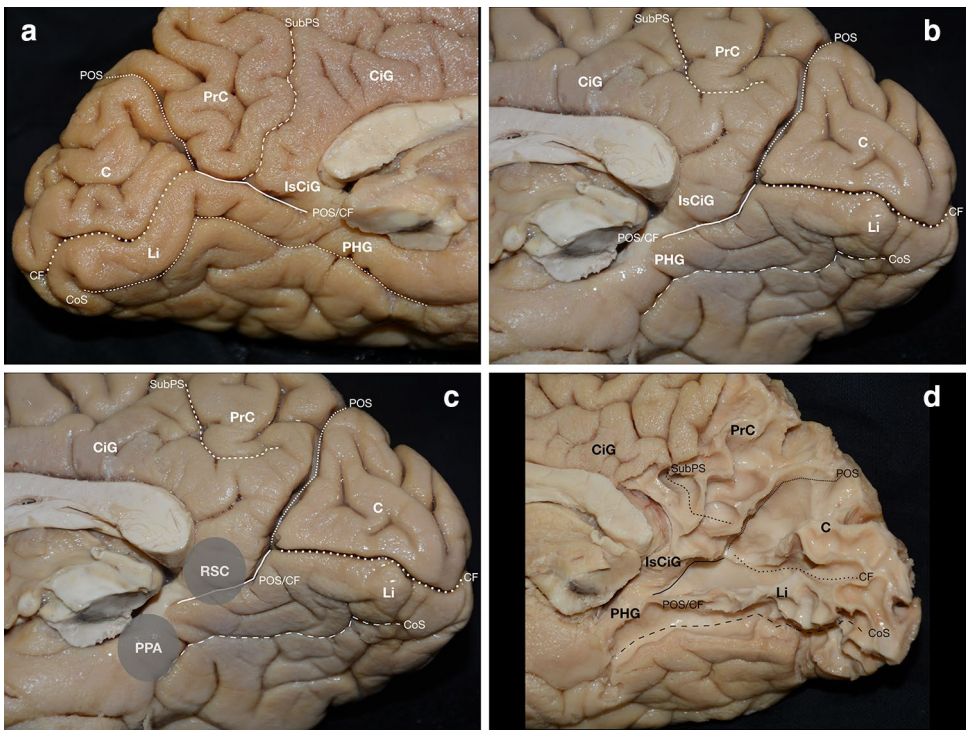

Fig. 1 Sulcal and gyral anatomy of the medial and basal cerebral surface of a left (**a**) and right (**b**) hemisphere. The parieto-occipital sulcus (demarcating the precuneus, isthmus of the cingulate gyrus and cuneus), the calcarine fissure (demarcating the cuneus and the lingual gyrus), their common stem (demarcating the lingula posterior parahippocampal gyrus and the isthmus of the cingulate gyrus), the collateral sulcus (demarcating the parahippocampal and fusiform gyri) and sub-parietal sulcus (demarcating the isthmus of the cingulate gyrus and the precuneus) are illustrated. **c** The cerebral areas known as the Retrosplenial Cortex (RSC) and Parahippocampal Place Area are demarcated in the specimen shown in **b** to correlate the anatomical landmarks to their functional equivalent. **d** The arcuate or U fibers of the medial surface of a right hemisphere are depicted. The plane of the parieto-occipital sulcus, calcarine fissure, their common stem and sub-parietal sulcus is marked for better orientation. *C* cuneus, *CiG* cingulate gyrus, *CF* calcarine fissure, *CoS* collateral sulcus, *IsCiG* isthmus of the cingulate gyrus, *Li* lingual gyrus, *PHG* parahippocampal gurus, *POS* parieto-occipital sulcus, *POS/CF* parieto-occipital sulcus and calcarine fissure common stem, *PPA* parahippocampal place area, *PrC* precuneus, *RSC* retrosplenial cortex, *SubPS* sub-parietal sulcus

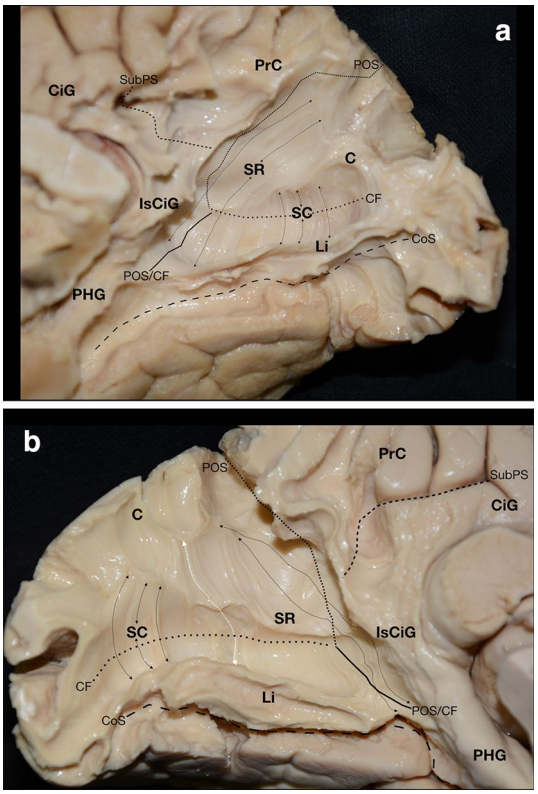

Fig. 2 Dissecting the U-fibers of a right (**a**) and a left (**b**) hemisphere reveals the fibers of the sledge runner fasciculus (SRF), the fibers of the cingulum arching over the splenium of the corpus callosum and a group of vertically oriented fibers located at the depth of the calcarine fissure, corresponding to the tract known as the "stratum calcarinum". **a** Right hemisphere: the SRF is seen to course in an oblique direction- just under the U-fibers of the medial cerebral surface-connecting the cuneus, the anterior part of the lingual gyrus, the cingulate isthmus and the posterior part of the parahippocampal gyrus. Note the fibers of the stratum calcarinum connecting the superior and inferior banks of the calcarine fissure. The direction and trajectory of the SRF and stratum calcarinum (SC) are marked with curved arrows. This white matter morphology of both the SRF and SC was consistently encountered in all studied specimens. **b** Left hemisphere: The anatomical silhouette of the SRF and SC is delineated with curved arrows. Note how the most anterior fibers of the SRF cross the plane of the parieto-occipital sulcus as they travel ventrally towards the isthmus of the cingulum and posterior part of the parahippocampal gyrus. Note also the clear anatomical boundary between the fibers of the SRF and SC in this specimen (distance between the most anterior black curved arrows placed on th SC and the posteriorly placed white arrow on the SR). *C* cuneus, *CiG* cingulate gyrus, *CF* calcarine fissure, *CoS* collateral sulcus, *IsCiG* isthmus of the cingulate gyrus, *Li* lingual gyrus, *PHG* parahippocampal gurus, *POS* parieto-occipital sulcus, *POS/CF* parieto-occipital sulcus and calcarine fissure common stem, *PrC* precuneus, *SC* stratum calcarinum, *SRF* sledge runner fasciculus, *SubPS* Sub-parietal sulcus

(Principal Investigators: Bruce Rosen, M.D., Ph.D., Martinos Center at Massachusetts General Hospital; Arthur W. Toga, Ph.D., University of Southern California, Van J. Weeden, MD, Martinos Center at Massachusetts General Hospital) is supported by the National Institute of Dental and Craniofacial Research (NIDCR), the National Institute of Mental Health (NIMH) and the National Institute of Neurological Disorders and Stroke (NINDS). HCP is the result of efforts of co-investigators from the University of Southern California, Martinos Center for Biomedical Imaging at Massachusetts General Hospital (MGH), Washington University, and the University of Minnesota.

Thirty-five healthy participants [mean age 31.1 years, (20–59 years old); 16 females/19 males] from the MGH-USC Adult Diffusion Dataset (Human Connectome available dataset) underwent brain imaging in a 3-Tesla CONNECTOM magnetic resonance imaging (MRI) scanner (Setsompop et al. 2013) housed at the MGH/HST Athinoula A. Martinos Center for Biomedical Imaging with a custom-made 64-channel phased array head coil (Keil et al. 2013). Anatomic imaging was performed with a 1 mm isotropic Multi-echo Magnetization-Prepared Rapid Acquisition Gradient Echo three-dimensional T1-weighted sequence. DTI parameters included an axial spin-echo multiband echo-planar imaging sequence with 64 diffusion encoding directions; field of view: 210 mm; acquisition voxel size: $1.5 \times 1.5 \times 1.5$ mm^3; repetition time: 8800 milliseconds; echo time: 57 milliseconds; *b* factors with 0 s/mm^2 (low *b* value) and 1000 s/mm^2 (high *b* value). The acquisition consisted of 96 slices.

DTI images were processed by the Brainance™ DTI Suite (Advantis Medical imaging, Eindhoven, The Netherlands). We applied a multiple region-of-interest (ROI) approach (Fig. 3) based on anatomical landmarks derived from previous white matter fiber dissection studies and the high signal intensity of the expected SR on fractional anisotropy (FA) maps. Tracing of the ROIs was performed in the axial (ROI 1 and ROI 2) and the coronal (ROI 3, ROI 4, ROI 5) planes, utilizing five different slices and the ROIs were placed based on discrete anatomical boundaries (Petrides 2012). For the first ROI, the parieto-occipital sulcus was identified in a sagittal plane, where the trajectory of the sledge runner could be also identified as a continuous tract on FA map (Fig. 3). Then, an axial plane was selected at the level of the lateral ventricles where the genu and the splenium of the corpus callosum were clearly distinguishable (upper 1/3 of the parieto-occipital sulcus); ROI 1 included a circular ROI placed just posterior to the cingulate sulcus (Fig. 3). The second ROI was placed in the axial plane, below the first slice, at a level where the posterior part of the insula and only the caudate nucleus among the basal ganglia were clearly identified; ROI 2 included a circular ROI covering a similar region as ROI 1 posterior to the cingulate sulcus (Fig. 3). For the third ROI, the mid part of the parieto-occipital sulcus was identified in the sagittal plane and a circular ROI was placed in the coronal plane covering the cerebral area demarcated by the posterior part of the calcarine sulcus and the white matter included between the lingual sulcus and the collateral sulcus (Fig. 3). The fourth

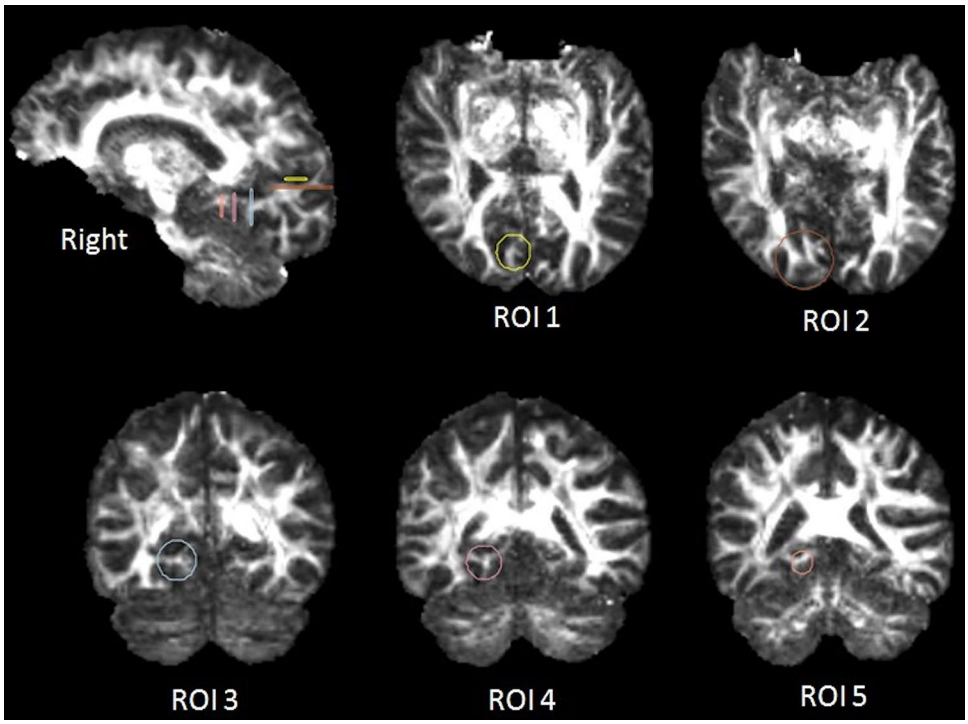

Fig. 3 Representation of the multiple ROIs used for the reconstruction of the SRF and projection over an FA map. *ROI* region of interest, *SRF* sledge runner fasciculus, *FA* fractional anisotropy

ROI was selected in the coronal plane at a level posterior to the splenium of the corpus callosum, where a part of the SRF medially to the lateral ventricle, below the calcarine sulcus and above the collateral sulcus/occipital ramus was identified (Fig. 3). The fifth and most anterior ROI was selected at the level of the middle part of the splenium of the corpus callosum, where a region of the SRF under the corpus callosum (medial to the lateral ventricles, below the calcarine sulcus and above the collateral sulcus/occipital ramus) was identified with a circular ROI (Fig. 3). All ROIs in individual space for each subject as well as subjects' DWI are available as supplementary material (DWI_ROIs_all_subjects.zip folder contains 35 folders, one per subject. Each folder contains three .nii files (DWI and ROI data). ROIs files have been named based on the following convention. The first four digits correspond to the ID number of each subject of the MGH-USC Adult Diffusion Dataset (Human Connectome available dataset). The next two digits, i.e. "SR", refer to the sledge runner fasciculus and the last digit corresponds to the left and right hemisphere). All tracts passing through these ROIs with a minimum FA of 0.15, maximum angle change of 90°, minimum length of 0 mm and maximum length of 200 mm were traced. The following DTI measures were then extracted for the right and left SRF: mean fractional anisotropy (FA); mean axial diffusivity (AD); mean radial diffusivity (RD); minimum, maximum and mean length; number of fibers (NoF). With regard to the topography of SRF in relation to adjacent white matter tracts, we further reconstructed the following tracts: forceps major, cingulum bundle, hippocampal—cingulum pathway, inferior longitudinal fasciculus. The reconstruction was based on a previous well-standardized protocol (Wakana et al. 2007) and Brainance™ DTI Suite default threshold values for FA, angle change and fiber length.

DTI data of ten participants were analyzed twice by a single experienced rater (E. K.) with an interval of 4 weeks, to assess intra-observer agreement. To determine inter-observer agreement for the SRF, the same dataset was additionally analyzed by a second experienced rater (F. C.), who was blinded to the results of the first rater. Intra- and inter-rater agreement (Table 1) was evaluated within the group of healthy participants with intraclass correlation coefficients (ICC) with an ICC greater than 0.75 being indicative of good agreement (Shrout and Fleiss 1979).

Results

Microanatomic dissection

A medial to lateral microanatomic fiber dissection focused on the area of the cuneus, lingual gyrus, posterior half of precuneus, isthmus of the cingulate gyrus and posterior parahippocampal gyrus was employed to study and record the morphology, connectivity and correlative topographic anatomy of the sledge runner fasciculus (Fig. 1). Initially, peeling away the cortex of the aforementioned gyri exposes the arcuate or U fibers (Fig. 1). Progressive dissection of the regional U fibers reveals the Sledge Runner fasciculus

Table 1 Indices of intra- and inter-rater agreement for SRF DTI measures for the group of healthy participants

SRF DTI measures	Intra-rater ICC	Inter-rater ICC
Left SRF		
FA	0.997	0.948
AD	0.999	0.939
RD	0.998	0.942
Max length	0.996	0.961
Min length	0.998	0.911
Mean length	0.999	0.992
NoF	0.912	0.843
Right SRF		
FA	0.998	0.981
AD	0.996	0.956
RD	0.999	0.939
Max length	0.995	0.992
Min length	0.997	0.944
Mean length	0.989	0.973
NoF	0.943	0.964

SRF sledge runner fasciculus, *DTI* diffusion tensor imaging, *ICC* intraclass correlation coefficient, *FA* fractional anisotropy, AD axial diffusivity, *RD* radial diffusivity, *Max* maximum, *Min* minimum, *NoF* number of fibers

along with fibers arching from the cingulum over the splenium of the corpus callosum (distal part of the superior arm and proximal part of the inferior arm of the cingulum). A distinct group of fibers exhibiting a vertical trajectory and encountered at the depth of the calcarine fissure correspond to the tract previously described by H.Sachs and known as "stratum calcarinum" (Fig. 2).

Connectivity and morphology of the sledge runner fasciculus (SRF)

The sledge runner fasciculus (SRF) was consistently identified as an oblique band of fibers travelling under the U-fibers of the medial surface of the occipital lobe, connecting the areas of the anterior cuneus, anterior half of the lingual gyrus, cingulate isthmus and posterior parahippocampal gyrus (Fig. 2). With respect to its trajectory and configuration, the SRF demonstrated a dorsomedial–ventrolateral direction with two medial curves—one at the level of the major forceps and the other at the inferior margin of the medial wall of the ventricular atrium- thus, creating its peculiar sled-like shape (Fig. 4). It was also consistently found to exhibit a superior narrow part, corresponding to the antero-superior part of the cuneus, which was seen to widen progressively as the tract descended towards the lingual gyrus (Fig. 4). The average length of the SRF was 4.9 cm (range 4.7–5.2 cm), while its average width was 1.7 cm (range 1.3–2) at its narrowest and 2,1 cm (range 1.8–2.5) at its widest part.

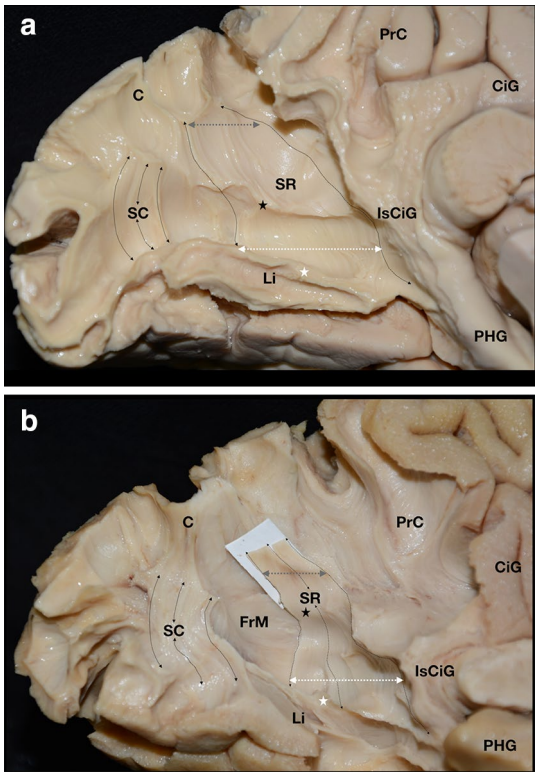

Fig. 4 **a, b** The morphology and configuration of the SRF is illustrated in two left hemispheres. The standard and consistent dorsomedial–ventrolateral direction of the SRF is depicted in both specimens. Note how the tract progressively widens from its dorsal narrow part, corresponding to the area of the cuneus (marked with the grey arrow), to its wider ventral part at the area of the cingulum and posterior parahippocampal gyrus (marked with the white arrow). During its course the SRF usually exhibits two medially directed curves, as seen and marked with black and white stars in these specimens. In the specimen included in **b**, we preserved the fibers of the SRF (marked with the white strap) while deepening the dissection plane posteriorly and exposing the more medially located fibers of the forceps major, thus illustrating the upper curve to lie at the level of the major forceps (marked in both specimens with the black star). The lower curve, marked with the white star, roughly corresponds to the level of the infero-medial wall of the ventricular atrium. *C* cuneus, *CiG* cingulate gyrus, FrM forceps major, *IsCiG* isthmus of the cingulate gyrus, *Li* lingual gyrus, *PHG* parahippocampal gurus, *PrC* precuneus, *SC* stratum calcarinum, *SRF* sledge runner fasciculus

SRF correlative anatomy with respect to the medial surface sulci and gyri

The characteristic aforementioned silhouette of the sledge runner fasciculus places its superior fibers in a deep plane just posterior to the superior two-thirds of the parieto-occipital sulcus. As the bundle travels anteriorly, to connect the area of the cuneus with the isthmus of the cingulate gyrus, its respective fibers are found deep at the level of the inferior

one-third of the parieto-occipital sulcus. There were no SRF fibers crossing the plane of the sub-parietal sulcus or entering the white matter of the precuneal lobule.

Deep to the calcarine fissure, the SRF fibers were seen to cross the distal part of the fissure in an almost vertical fashion, connecting the cuneus with the anterior half of the lingual gyrus. In relation to the common trunk formed by the proximal parts of the calcarine fissure and the parieto-occipital sulcus, the SRF fibers course in an almost parallel fashion deep to the trajectory of the sulcus, extending both superiorly and inferiorly to reach the level of the cingulate isthmus and posterior part of the parahippocampal gyrus, respectively (Fig. 2). With respect to the regional gyral anatomy, the SRF lies deep at the level of anterior half of cuneus, anterior half of the lingual gyrus, isthmus of cingulate gyrus and posterior part of parahippocampal gyrus.

SRF Subcortical correlative anatomy

We observed the fibers of the cingulum lying adjacent to the fibers of the SRF. This relation was particularly tight with regard to the most anteroinferior part of the SRF, which runs deep to the isthmus of the cingulate gyrus and posterior part of the parahippocampal gyrus. To clarify and illustrate more vividly the regional anatomy, we dissected this part of the sledge runner fasciculus and we further observed that it lies medial and posterior to the fibers of the cingulum, displaying a postero-supero-medial to antero-infero-lateral direction while the cingulum fibers travel antero-supero-medially to postero-infero-laterally. (Fig. 5).

Deep to the plane of the calcarine fissure, we consistently observed a distinct group of vertically oriented fibers known as the stratum calcarinum, running between the upper and lower banks of the fissure and connecting the upper and lower lips of the calcarine cortex. This elegant tract lies posterior to the SRF and in 60% of the studied specimens (12/20) it exhibits a clear demarcation from the SRF (Fig. 4). In the remaining 40% of hemispheres (8/20) this tract was seen to intermingle with the fibers of the SRF anteriorly, displaying however a different orientation and trajectory (vertical for the SC vs. oblique for the SRF) (Fig. 6).

Gradual dissection of the SRF reveals the fibers of the forceps major, running from the splenium of the corpus

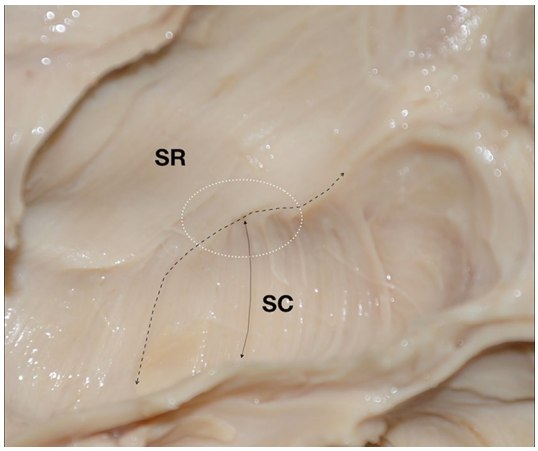

Fig. 6 High magnification of the regional anatomy of a right hemisphere at the level of the SRF and SC fasciculi i.e. just under the U fibers of the medial surface of the occipital lobe. Note the tight anatomical relationship between the fibers of the SR and SC illustrated with the white circle. Continuous and dashed arrows delineate the trajectory of the SR and SC respectively. *SC* stratum calcarinum, *SRF* sledge runner fasciculus

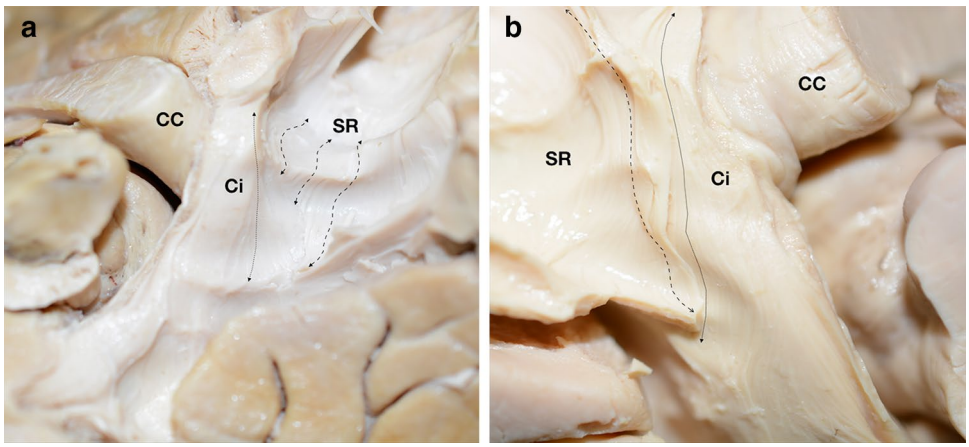

Fig. 5 Photos of a right (**a**) and left (**b**) cerebral hemisphere zooming in the correlative topography of the SRF with regard to the fibers of the cingulum. In both figures, the anatomical vicinity between the most anteriorly descending fibers of the SRF and the fibers of the inferior arm of the cingulum is illustrated. The different trajectories of the aforementioned fibers are marked with arrows. Note that the SRF travels in a postero-supero-medial to antero-infero-lateral direction while the fibers of the cingulum take an antero-supero-medial to postero-infero-lateral course. *CC* corpus callosum, *Ci* cingulum, *SR* Sledge runner fasciculus

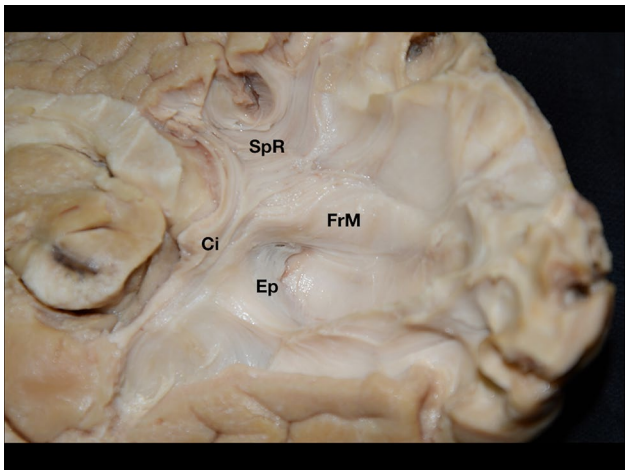

Fig. 7 Oblique view of a right hemisphere. Gradual white matter dissection exposes the fibers of the major forceps and the ventricular ependyma of the medial wall of the atrium. *Ci* cingulum, *Ep* ependyma, *FrM* forceps major, *SpR* splenial radiations

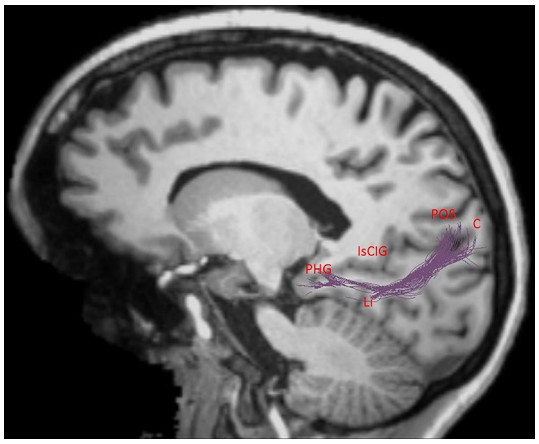

Fig. 8 Representation of the trajectory of the right SRF for a healthy participant and projection over an anatomical 3D high-resolution T1 weighted image (sagittal plane). *SRF* sledge runner fasciculus, *POS* parieto-occipital sulcus, *C* cuneus, *IsCIG* cingulate isthmus, *PHG* parahippocampal gyrus, *Li* lingual gyrus

callosum towards the medial wall of the atrium and occipital horn (Fig. 7). By removing the forceps major and the subsequently encountered ventricular ependyma we finally enter the atrium and occipital horn. During this process we observed the superior part of the SRF lying medially and coursing almost vertically in relation to the location and trajectory of the forceps major while the inferior SRF part was always found to correspond to the medial wall of the atrium.

DTI imaging

The applied multi-ROI tractography protocol was successful for the reconstruction of the SRF and the extracted results were in line with the trajectory, direction and connectivity of the SRF fibers found during the white matter fiber dissection part of the study. The reconstructed SRF for a single subject is superimposed on a sagittal 3D T1 weighted image (Fig. 8), where the trajectory of the SRT along the anterior cuneus, anterior part of the lingual gyrus and posterior parahippocampal gyrus is delineated. We failed to reconstruct the left SRF in one subject with the predefined thresholds for FA, angle threshold and step size.

DTI indices and CV% are presented in Table 2. The variability of the reconstructed tracts for the left and right hemispheres for all participants is depicted by CV%.

To further delineate the SRF white matter topography, we also reconstructed the forceps major, the cingulum bundle, the hippocampal–cingulum pathway and the inferior longitudinal fasciculus. Figure 9 depicts the anatomy of SRF in association with the adjacent white matter tracts in one subject.

Discussion

Although many texts and atlases have previously investigated the anatomy and fiber tract morphology of the occipital lobe (Catani et al. 2002; Fernandez-Miranda et al. 2008a; Mamata et al. 2002; Mori et al. 1999, 2005; Ture et al. 2000; Koutsarnakis et al. 2015; Catani and de Schotten 2012; Alves et al. 2012; Forkel et al. 2014; Thiebaut de Schotten et al. 2014; Schmahmann and Pandya 2009; Sachs 1892; Catani and Thiebaut de Schotten 2008), it was not until the publication of the laboratory anatomical report by Vergani and colleagues entitled "Intralobar fibres of the occipital lobe: A post mortem dissection study" in which the authors identified a novel fiber bundle that was not previously described and named it "sledge runner fasciculus" after its peculiar shape (Vergani et al. 2014). In this study the authors explored the white matter architecture of the occipital lobe in three cadaveric hemispheres through the fiber dissection (Klingler's) technique and compared their results to the anatomic atlas written by H.Sachs "The hemispheric white matter of the human brain. Part I: The occipital lobe" (Sachs 1892). During their dissections they found a very close concordance between the histological preparations of Sachs and the Klingler's technique that they used, with the only difference being the identification of an unrecognized fiber pathway located in a plane deep to the calcarine fissure. However, Vergani and colleagues did not proceed to a more detailed description of this tract in terms of morphology, topography and connectivity since it was out of the scope of their manuscript. Since then, there have been only two published anatomo-tractographic studies entitled "The white matter tracts of the cerebrum in ventricular surgery and hydrocephalus" by Gungor et al. (2017) and "Fiber

Table 2 DTI indices of bilateral sledge runner fasciculus reconstructions

SRF DTI measures	Left SRF	CV%	Right SRF	CV%
FA	0.41 ± 0.04	9.76	0.41 ± 0.03	7.32
AD	$1.24 \times 10^{-3} \pm 0.09 \times 10^{-3}$	7.26	$1.23 \times 10^{-3} \pm 0.07 \times 10^{-3}$	5.69
RD	$0.65 \times 10^{-3} \pm 0.06 \times 10^{-3}$	9.23	$0.65 \times 10^{-3} \pm 0.06 \times 10^{-3}$	9.23
Mean length	67.77 ± 11.30	16.67	66.50 ± 10.14	15.25

SRF sledge runner fasciculus, *DTI* diffusion tensor imaging, *FA* fractional anisotropy, *AD* axial diffusivity, *RD* radial diffusivity, *CV* coefficient of variation

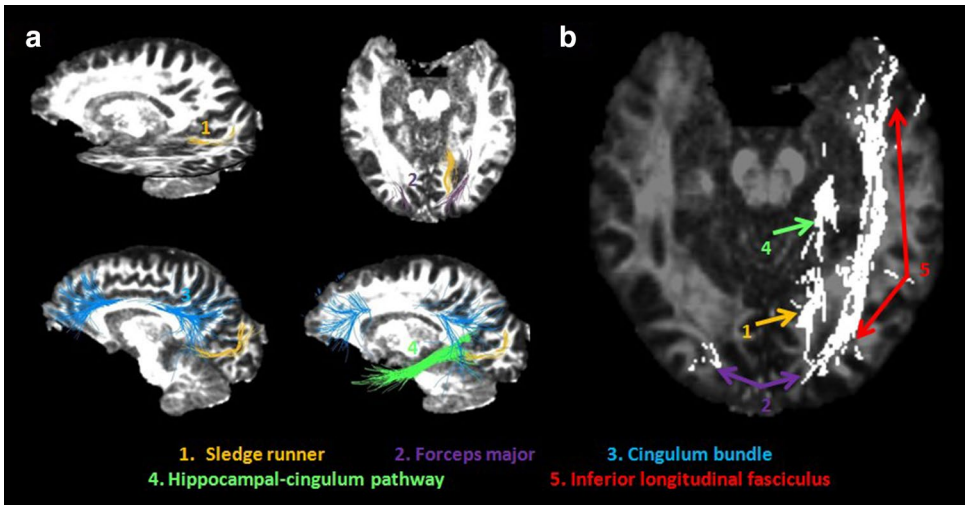

Fig. 9 Representation of the topography of SRF (colored in yellow) in association with adjacent white matter tracts [cingulum bundle (colored in blue); hippocampal-cingulum pathway (colored in green); forceps major (colored in purple); inferior longitudinal fasciculus (colored in red)] and projection over a FA image (sagittal/axial plane). *SRF* sledge runner fasciculus, *FA* fractional anisotropy

Tracts of the Medial and Inferior Surfaces of the Cerebrum" by Baydin et al. (2017) that refer to this fiber tract, but again the anatomic descriptions provided are not detailed due to the more generic objective of these laboratory investigations.

In this context, the present study attempts to address this gap and enhance anatomical knowledge regarding the sledge runner fasciculus (SRF) through cadaveric white matter dissections combined with a DTI protocol carried out in a public available dataset from the HCP. Additional available ROIs in individual space, descriptive measures and degree of variability for the most commonly used DTI metrics are also provided. DTI based tractography is a sophisticated neuroimaging technique widely used to reconstruct and noninvasively map the cerebral white matter architecture. It is however prone to anatomic inaccuracies and artifacts, particularly when applied to complex subcortical areas, related not only to the MR noise but also to the crossing, kissing and bending effect of the fiber tracts and thus it is deemed unfit to discover and describe new white matter pathways (Oouchi et al. 2007; Vos et al. 2011; Johansen-Berg and Rushworth 2009; Le Bihan et al. 2006; Fernandez-Miranda et al. 2012; Tournier et al. 2012.) We therefore opted to combine DTI tractography with the fiber microdissection technique, which is considered the gold standard method for investigating novel fiber tracts and is used to validate evidence coming from DTI studies (Zemmoura et al. 2016; Silva and Andrade 2016). More specifically, 20 normal adult cadaveric hemispheres were dissected using the Klingler's technique and the microscope and 35 normal individuals with available DTI data from the HCP were analyzed using ROI-based DTI tractography, with the aim to describe in detail the topography, morphology and connectivity of this elegant fiber tract, establish the degree of correspondence between microanatomic dissection and in vivo tractography findings and provide descriptive DTI measures for the SRF. We therefore consistently identified the SRF as a distinct white matter pathway lying under the U fibers of the medial occipital lobe, exhibiting an oblique dorsomedial–ventrolateral direction and connecting the areas of the anterior cuneus, anterior lingula, isthmus of the cingulum and posterior parahippocampal gyrus. It originates as a relatively narrow tract, at the area of the cuneus, and during its course, it fans out and progressively widens as it descends towards the parahippocampal region, displaying two medial curves at the level of the forceps major and inferior part of the ventricular atrium respectively. With regard to its topography, the SRF was seen to cross the plane of the calcarine fissure and that of the common trunk formed by the calcarine fissure and parieto-occipital sulcus, thus connecting the cuneus to the lingula and posterior parahippocampal region, while it was observed to course deep to the proximal 1/3 of the parieto-occipital sulcus, connecting the cuneus to the isthmus of the

cingulum. It was consistently found not to cross the plane of the sub-parietal sulcus or to enter the white matter of the precuneal lobule. The fibers of the SRF lie in the same plane and just anterior to the fibers of the stratum calcarinum, a vertically oriented white matter tract that connects the upper and lower lips of the calcarine cortex that has been previously described in the anatomic atlas of H. Sachs (Sachs 1892). The two tracts display a clear boundary in 60% of studied specimens, while in the remaining 40% they were observed to progressively intermingle in their ventral projection, exhibiting however a different trajectory, which aids in their proper identification and differentiation. Due to this elegant morphology, these fiber pathways should be carefully identified and dissected since anatomic misinterpretation can very easily occur. Topographically and in deeper dissection plane, the dorsal part of the SRF was found to correspond to the forceps major while its ventral part to the medial wall of the ventricular atrium.

A particularly tight anatomic relationship between the SRF and the cingulum bundle at the area of the cingulate isthmus, just posterior to the splenium of the corpus callosum was revealed in our dissections. The cingulum bundle is a white matter tract which encircles the corpus callosum and through its radiations supports the connection of the frontal, temporal and parietal lobes (Jones et al. 2013a; Wu et al. 2016). In particular, the posterior projection of this bundle known as posterior cingulum (Ito et al. 2015) or parahippocampal cingulum (Jones et al. 2013a) or Cingulum Bundle V (Wu et al. 2016) connects the parahippocampal gyrus with the precuneus (Baydin et al. 2017). As such, to reach the precuneus, the cingulum travels in the depth of the parahippocampal gyrus and cingulate isthmus sharing a similar trajectory with the sledge runner at this level. In this context, we aimed to elucidate this relationship by heavily focusing our dissections on the specific areas. We observed that as the SRF courses deep to the cingulate isthmus it lies superficially (medially) to the cingulum fibers with a postero-supero-medial to antero-infero-lateral direction while the cingulum fibers course from antero-supero-medially to postero-infero-laterally before they arch over the splenium of the corpus callosum (Fig. 5). Moreover, the termination fibers of the SRF were encountered at the posterior part of the parahippocampal gyrus while the cingulum was observed to continue its course towards the anterior temporal lobe (Fig. 5).

Regarding the in vivo reconstruction of the SRF, we applied a multi-ROI protocol in publicly available data from the HCP, which is fully described for replication and yielded high intra- and inter-rater reliability for the examined DTI indices. We also used a robust DTI algorithm, which has been previously shown to be reliable for the reconstruction of white matter tracts including fibers (e.g. lateral cortical projections and crossing pontine fibers of the corticospinal tract) that cannot be reconstructed with previous deterministic algorithms (Christidi et al. 2016). By qualitatively comparing dissection and tractography findings, our study provides evidence of similar findings concerning the anatomical trajectory of the SRF (i.e. connections between the anterior cuneus, anterior lingual, isthmus of the cingulate gyrus and posterior parahippocampal gyrus) and its topography in relation to adjacent white matter tracts (i.e. cingulum bundle, hippocampal–cingulate pathway, forceps major). However, using predefined thresholds, we failed to reconstruct the left SRF in one subject; by applying different thresholds by means of FA and angle degree, the resulted tract was considered erroneous and unreliable (e.g. false-positive). The tracking of the SRF is challenging because of the turning angle and the curving features along its course as well as fiber intercrossing. Elevated CV% of DTI metrics might indicate the complexity of the SRF reconstruction. System—(e.g. B0 inhomogeneity or gradient non-linearity) or radiographer—(e.g. subject positioning, slice tilt) related factors can contribute to the increased intersubject variation. However, in a well-designed study where system—and user-related errors had been minimized, there was increased variability in DTI indices using ROIs measures in different brain anatomical structures (Veenith et al. 2013) which is in line with previous studies (Bisdas et al. 2008; Danielian et al. 2010; Heiervang et al. 2006; Takao et al. 2012). In our study, the calculated CV% values of FA, AD and RD metrics are in accordance with previous studies. The above-mentioned findings as well as the high complexity of SRF and the high intra- and inter-observer agreement strengthen the reliability of our findings. A multimodal task-related fMRI-DTI study is definitely warranted to fully describe the structural trajectory and the functional role of SRF.

From an anatomical–functional point of view, we reconstructed a white matter tract which was so far under-recognized as a distinct white matter tract, has a significant functional role and its anatomical trajectory includes regions that are often involved in neurosurgical procedures. The reconstruction of white matter tracts in everyday radiological practice is often hampered by low-resolution DWI sequences which were initially included in the clinical protocols to exclude and/or identify recently onset vascular lesions and not to reconstruct specific white matter tracts and especially those that are highly relied on non-low resolution DTI data. In our study, we applied a DTI reconstruction algorithm which has previously led us to reliably reconstruct not only common associative white matter tracts such as the uncinate fasciculus but also the hippocampal perforant pathway (Christidi et al. 2017) and the ipsilateral/contralateral cortico-cerebellar connections (Karavasilis et al. 2018). Tractography protocols are applied using manually placed or atlas-based ROIs. Even though using atlas-based ROIs created in a standard space such

as MNI can be easily used to compare between subjects or studies (Froeling et al. 2016), this approach cannot be applied in misaligned data or in white matter tracts with significant anatomical variations (such as the one examined in our study). The main purpose of our study was to identify the SRF using a reconstruction protocol that can be further used by experienced or non-experienced DTI users in clinical and research practice using available DTI platforms provided either by the MRI scanner manufacturers or other companies. Thus, by providing a detailed description of the anatomical trajectory of SRF on DTI data with a public access (i.e. Human Connectome Project) and the identification of multiple ROIs which are publicly available in individual space, our protocol might be helpful for both experienced and non-experienced raters on the identification and reconstruction of SRF.

Given its subcortical architecture, the SRF was consistently recorded to connect the cortices of the anterior cuneus, anterior lingula, isthmus of the cingulate gyrus and posterior parahippocampal gyrus in all studied hemispheres. Growing body of evidence suggests that these cerebral areas are primarily involved in the perception of complex visual scenes and in the recovery of familiar spatial knowledge, thus subserving spatial memory, wayfinding and visuospatial imagery (Whittingstall et al. 2014; Epstein et al. 2001, 2007a, b, 2017; Epstein 2008; Ino et al. 2002; Epstein and Kanwisher 1998; Spiers and Maguire 2006, 2007; Aguirre and D'Esposito 1999; O'Craven and Kanwisher 2000; Barrash et al. 2000; Pallis 1955; Maguire et al. 1997; Henderson et al. 2008; Sugiura et al. 2005; Wolbers and Buchel 2005). More specifically, the posterior part of the parahippocampal gyrus, widely known in neuropsychology as the parahippocampal place area (PPA), has been documented through functional imaging and stroke studies to activate strongly to complex landscapes and cityscapes, mainly by encoding the main spatial outline of the scene (Epstein et al. 2001, 2007b, 2017; Epstein 2008; Knauff et al. 2000). To this end, the PPA seems to respond to a large topographical entity by treating it in a unified manner i.e. as a single discrete object, in contrast to hippocampal activity, which primarily encodes information about specific objects and their respective spatial location within a certain landscape, thus supporting a concept of double dissociation between scene and object recognition (Janzen and van Turennout 2004; Lee et al. 2005; King et al. 2002; Goh et al. 2004; Buffalo et al. 2006). Interestingly, PPA activity is not exclusively dependent on visual stimuli but can also be triggered by scenes and landscapes brought in mind during mental navigation tasks (O'Craven and Kanwisher 2000; Maguire et al. 1997; Bridge et al. 2012; Rosenbaum et al. 2004).

The cerebral territory, in turn, demarcated by the anterior lingula, anterior cuneus and cingulate isthmus, collectively referred as the retrosplenial cortex (RSC) in the field of neurocognitive research, has been documented to respond mainly to familiar topographical entities (Ino et al. 2002; O'Craven and Kanwisher 2000; Epstein et al. 2007b). Indeed, RSC is involved in the recovery of familiar spatial knowledge thus participating in the neural circuit of long term spatial memory (Epstein et al. 2007a; Sugiura et al. 2005; Vann et al. 2009). In addition, evidence from fMRI studies indicates that the retrosplenial cortex also activates when subjects imagine orienting and navigating themselves in familiar places, hence playing a significant role in integrating visuospatial imagery (Whittingstall et al. 2014; Epstein et al. 2017; Epstein 2008; Ino et al. 2002; O'Craven and Kanwisher 2000; Knauff et al. 2000; Rosenbaum et al. 2004). As such, damage to this brain area results in wayfinding and orientation issues, whereas lesions confined to the PPA manifest with difficulties in encoding the topographical structure and layout of newly introduced landscapes (Aguirre and D'Esposito 1999; Barrash et al. 2000; Pallis 1955; Hecaen et al. 1980; Takahashi et al. 1997; Ino et al. 2007; Katayama et al. 1999; Bottini et al. 1990; Osawa et al. 2008; Ploner et al. 2000).

Whether these two distinct but functionally complementary cortical regions are directly connected through a subcortical network or act alternatively as key hubs that promote an indirect connectivity between distant cerebral areas, has been a topic of recent research (Whittingstall et al. 2014; Epstein et al. 2017; Beyh et al. 2017; Powell et al. 2004; Malykhin et al. 2008; Catani et al. 2003). To this end, the implementation of methodological advances in diffusion MRI (dMRI), such as the high angular resolution diffusion imaging (HARDI) protocol (Tournier et al. 2012; Descoteaux and Poupon 2012; Seunarine and Alexander 2014), along with the use of fMRI–dMRI techniques (Gong et al. 2009; Hagmann et al. 2007; Honey et al. 2007; Johansen-Berg and Behrens 2006) have offered valuable insights into the structural connectivity of the neural correlates of spatial navigation and visuospatial imagery. Indeed, growing body of evidence points towards a common white matter pathway that directly links the cortical areas of interest i.e. the PPA and RSC (Whittingstall et al. 2014; Beyh et al. 2017; Kravitz et al. 2011). This fiber tract, allegedly conveying the core cognitive ability of spatial navigation and visuospatial imagery, has been described in a recent tractographic study and has been alternatively named as the medial occipital longitudinal tract (MOLT) (Beyh et al. 2017). Here, we provide anatomic and imaging data on the morphology and axonal connectivity of the SRF through microanatomic dissections and DTI tractography thus raising awareness on the structural architecture of this recently identified WM tract believed to participate in the neural circuit of spatial navigation and visuospatial imagery.

Study limitations

Magnetic resonance (MR) diffusion tractography is a sophisticated, in vivo, fast, non-invasive but indirect method to map the cerebral white matter architecture, based on the diffusion properties of water molecules along the direction of nerve axons. Anatomic data deriving from this technique can significantly vary due to various differences in acquisition and post processing parameters used (Mori and Zhang 2006; Jones and Cercignani 2010; Jones et al. 2013b; Nimsky et al. 2016; Thomas et al. 2014). Additionally, as already highlighted in the "Discussion" section, DTI tractography is prone to inaccurate results and artifacts, having the tendency to create erroneous white matter tracts, particularly when applied to narrow and anatomically complex cerebral areas, due to the crossing, kissing and bending effects as well as to the partial volume effect generated near CSF filled cavities (Oouchi et al. 2007; Vos et al. 2011; Johansen-Berg and Rushworth 2009; Le Bihan et al. 2006; Fernandez-Miranda et al. 2012; Tournier et al. 2012). For these reasons, DTI results and especially those regarding novel fiber tracts have to be fully validated through other more robust methods.

The Klingler's technique in turn, is used for the blunt dissection of white matter tracts and entails the fixation of cadaveric specimens in a formalin solution followed by a freeze-thaw process, during which the formation of ice crystals separates the white matter fibers thus rendering their dissection feasible. This method -first described by Klingler (1935) has been recently revived after a long period of neglect, mainly due to the advent of MR tractography. The question of whether this technique of formalin fixation and freezing- defrosting procedure alters the integrity of myelin sheaths and consequently interferes with the axonal ultrastructure has been thoroughly answered by Zemmoura et al. in their recently published study (Zemmoura et al. 2016). The authors have proved that the Klingler's preparation method maintains the white matter axonal integrity and structure, interfering only with the extracellular matrix, and therefore the results obtained are accurate. Hence, Klingler's dissection is considered the gold standard technique for testing the validity of DTI studies.

Apart from being a very delicate, operator dependent, time consuming procedure the Klingler's technique offers lower spatial resolutions in comparison to histology, polarized light imaging and optical coherence tomography, maintaining on the contrary the three-dimensional coherence of the white matter tracts (Dammers et al. 2010; Goergen et al. 2012; Magnain et al. 2014; Palm et al. 2010; Wang et al. 2011). Most significant however is the fact that by the Klingler's method one is unable to simultaneously investigate tracts that exhibit fibers with crossing directions since the proper dissection of the one means the destruction of the other. Lastly, it remains ambiguous whether the cortical terminations of the white matter pathways can be adequately demonstrated through this technique, even though recent studies have reported so (Martino et al. 2013; Sarubbo et al. 2013).

Conclusion

Laboratory white matter dissections and DTI studies were employed with the aim to investigate and record the structural architecture of a fiber tract residing in the medial part of the occipital lobe known as the SRF. By combining the Klingler's dissection method and a reliable DTI protocol with public available ROIs on dataset from the HCP yielding high intra- and inter-rater agreement values and providing descriptive and variability measures for DTI indices, our results support the hypothesis that the SRF is consistently involved in the axonal connectivity of cerebral areas that are believed to be strongly implicated in the cognitive ability of spatial navigation and visuospatial imagery.

Author contributions Conception and design: CK, AVK. Acquisition of data: AVK, CK, GPS, FC, EK, NK, GV. Analysis and interpretation of data: AVK, CK, FC, EK, NK, FL, JE, ZG. Drafting the article: CK, AVK, FC, EK. Critically revising the article: CK, AVK, SK, TK, FL, JE, GS. Reviewed submitted version of manuscript: All authors. Administrative technical, material support: GS. Study supervision: CK.

Funding No funding was received for this study.

Compliance with ethical standards

Conflict of interest The authors declare no conflict of interest regarding the materials or methods used in the current study or the findings specified in this paper.

Informed consent Informed consent was obtained from all participants included in the study.

References

Aguirre GK, D'Esposito M (1999) Topographical disorientation: a synthesis and taxonomy. Brain J Neurol 122(Pt 9):1613–1628

Alves RV, Ribas GC, Parraga RG, de Oliveira E (2012) The occipital lobe convexity sulci and gyri. J Neurosurg 116(5):1014–1023. https://doi.org/10.3171/2012.1.JNS11978

Arnts H, Kleinnijenhuis M, Kooloos JG, Schepens-Franke AN, van Cappellen van Walsum AM (2014) Combining fiber dissection, plastination, and tractography for neuroanatomical education: revealing the cerebellar nuclei and their white matter connections. Anat Sci Educ 7(1):47–55

Barrash J, Damasio H, Adolphs R, Tranel D (2000) The neuroanatomical correlates of route learning impairment. Neuropsychologia 38(6):820–836

Baydin S, Gungor A, Tanriover N, Baran O, Middlebrooks EH, Rhoton AL Jr (2017) Fiber tracts of the medial and inferior surfaces of the cerebrum. World Neurosurg 98:34–49. https://doi.org/10.1016/j.wneu.2016.05.016

Beyh A, Laguna Luque P, De Santiago Requejo F, Dell'Acqua F, Ffytche D, Catani M (2017) The medial occipital longitudinal tract: a white matter system for spatial navigation. In: Paper presented at the OHBM2017, Vancouver

Bisdas S, Bohning DE, Besenski N, Nicholas JS, Rumboldt Z (2008) Reproducibility, interrater agreement, and age-related changes of fractional anisotropy measures at 3T in healthy subjects: effect of the applied b-value. AJNR Am J Neuroradiol 29:1128–1133

Bottini G, Cappa S, Geminiani G, Sterzi R (1990) Topographic disorientation—a case report. Neuropsychologia 28(3):309–312

Bridge H, Harrold S, Holmes EA, Stokes M, Kennard C (2012) Vivid visual mental imagery in the absence of the primary visual cortex. J Neurol 259(6):1062–1070. https://doi.org/10.1007/s00415-011-6299-z

Buffalo EA, Bellgowan PS, Martin A (2006) Distinct roles for medial temporal lobe structures in memory for objects and their locations. Learn Mem 13(5):638–643. https://doi.org/10.1101/lm.251906

Catani M, de Schotten MT (2012) Introduction to diffusion imaging tractography. In: Catani M, de Schotten MT (eds) Atlas of human brain connections. Oxford University Press, New York

Catani M, Thiebaut de Schotten M (2008) A diffusion tensor imaging tractography atlas for virtual in vivo dissections. Cortex 44(8):1105–1132. https://doi.org/10.1016/j.cortex.2008.05.004

Catani M, Howard RJ, Pajevic S, Jones DK (2002) Virtual in vivo interactive dissection of white matter fasciculi in the human brain. Neuroimage 17(1):77–94

Catani M, Jones DK, Donato R, Ffytche DH (2003) Occipito-temporal connections in the human brain. Brain 126 (Pt 9):2093–2107. https://doi.org/10.1093/brain/awg203

Catani M, Jones DK, ffytche DH (2005) Perisylvian language networks of the human brain. Ann Neurol 57(1):8–16. https://doi.org/10.1002/ana.20319

Christidi F, Karavasilis E, Samiotis K, Bisdas S, Papanikolaou N (2016) Fiber tracking: a qualitative and quantitative comparison between four different software tools on the reconstruction of major white matter tracts. Eur J Radiol Open 3:153–161. https://doi.org/10.1016/j.ejro.2016.06.002

Christidi F, Karavasilis E, Zalonis I, Ferentinos P, Giavri Z, Wilde EA, Xirou S, Rentzos M, Zouvelou V, Velonakis G, Toulas P, Efstathopoulos E, Poulou L, Argyropoulos G, Athanasakos A, Zambelis T, Levin HS, Karandreas N, Kelekis N, Evdokimidis I (2017) Memory-related white matter tract integrity in amyotrophic lateral sclerosis: an advanced neuroimaging and neuropsychological study. Neurobiol Aging 49:69–78

Dammers J, Axer M, Gräßel D, Palm C, Zilles K, Amunts K, Pietrzyk U (2010) Signal enhancement in polarized light imaging by means of independent component analysis. Neuroimage 49:1241–1248

Danielian LE, Iwata NK, Thomasson DM, Floeter MK (2010) Reliability of fiber tracking measurements in diffusion tensor imaging for longitudinal study. Neuroimage 49:1572–1580

De Benedictis A, Duffau H (2011) Brain hodotopy: from esoteric concept to practical surgical applications. Neurosurgery 68(6):1709–1723. https://doi.org/10.1227/NEU.0b013e3182124690 **(discussion 1723)**

Descoteaux M, Poupon C (2012) Diffusion-weighted MRI. Compr Biomed Phys 3(6):81–97

Duffau H (2006) New concepts in surgery of WHO grade II gliomas: functional brain mapping, connectionism and plasticity—a review. J Neurooncol 79(1):77–115. https://doi.org/10.1007/s11060-005-9109-6

Duffau H (2011) Brain hodotopy: new insights provided by intrasurgical mapping. In: Duffau H (ed) Brain mapping. Springer, Wien, pp 335–347

Duffau H (2015) Stimulation mapping of white matter tracts to study brain functional connectivity. Nat Rev Neurol 11(5):255–265. https://doi.org/10.1038/nrneurol.2015.51

Duffau H (2017) Hodotopy, neuroplasticity and diffuse gliomas. Neurochirurgie 63(3):259–265. https://doi.org/10.1016/j.neuchi.2016.12.001

Duffau H, Capelle L, Sichez N, Denvil D, Lopes M, Sichez JP, Bitar A, Fohanno D (2002) Intraoperative mapping of the subcortical language pathways using direct stimulations. An anatomo-functional study. Brain 125(Pt 1):199–214

Duffau H, Gatignol P, Mandonnet E, Peruzzi P, Tzourio-Mazoyer N, Capelle L (2005) New insights into the anatomo-functional connectivity of the semantic system: a study using cortico–subcortical electrostimulations. Brain 128(Pt 4):797–810. https://doi.org/10.1093/brain/awh423

Duffau H, Moritz-Gasser S, Mandonnet E (2014) A re-examination of neural basis of language processing: proposal of a dynamic hodotopical model from data provided by brain stimulation mapping during picture naming. Brain Lang 131:1–10. https://doi.org/10.1016/j.bandl.2013.05.011

Epstein RA (2008) Parahippocampal and retrosplenial contributions to human spatial navigation. Trends Cogn Sci 12(10):388–396. https://doi.org/10.1016/j.tics.2008.07.004

Epstein R, Kanwisher N (1998) A cortical representation of the local visual environment. Nature 392(6676):598–601. https://doi.org/10.1038/33402

Epstein R, Deyoe EA, Press DZ, Rosen AC, Kanwisher N (2001) Neuropsychological evidence for a topographical learning mechanism in parahippocampal cortex. Cogn Neuropsychol 18(6):481–508. https://doi.org/10.1080/02643290125929

Epstein RA, Higgins JS, Jablonski K, Feiler AM (2007a) Visual scene processing in familiar and unfamiliar environments. J Neurophysiol 97(5):3670–3683. https://doi.org/10.1152/jn.00003.2007

Epstein RA, Parker WE, Feiler AM (2007b) Where am I now? Distinct roles for parahippocampal and retrosplenial cortices in place recognition. J Neurosci 27(23):6141–6149. https://doi.org/10.1523/JNEUROSCI.0799-07.2007

Epstein RA, Patai EZ, Julian JB, Spiers HJ (2017) The cognitive map in humans: spatial navigation and beyond. Nat Neurosci 20(11):1504–1513. https://doi.org/10.1038/nn.4656

Fernandez-Miranda JC, Rhoton AL Jr, Alvarez-Linera J, Kakizawa Y, Choi C, de Oliveira EP (2008a) Three-dimensional microsurgical and tractographic anatomy of the white matter of the human brain. Neurosurgery 62(6 Suppl 3):989–1026. https://doi.org/10.1227/01.neu.0000333767.05328.49 **(discussion 1026–1028)**

Fernandez-Miranda JC, Rhoton AL Jr, Kakizawa Y, Choi C, Alvarez-Linera J (2008b) The claustrum and its projection system in the human brain: a microsurgical and tractographic anatomical study. J Neurosurg 108(4):764–774. https://doi.org/10.3171/JNS/2008/108/4/0764

Fernandez-Miranda JC, Pathak S, Engh J, Jarbo K, Verstynen T, Yeh FC, Wang Y, Mintz A, Boada F, Schneider W, Friedlander R (2012) High-definition fiber tractography of the human brain: neuroanatomical validation and neurosurgical applications. Neurosurgery 71(2):430–453. https://doi.org/10.1227/NEU.0b013e3182592faa

Forkel SJ, Thiebaut de Schotten M, Kawadler JM, Dell'Acqua F, Danek A, Catani M (2014) The anatomy of fronto-occipital connections

from early blunt dissections to contemporary tractography. Cortex 56:73–84. https://doi.org/10.1016/j.cortex.2012.09.005
Froeling M, Pullens P, Leemans A (2016) DTI analysis methods: region of interest analysis. In: Van Hecke W et al (eds) Diffusion tensor imaging. Springer Science + Business Media, New York
Goergen CJ, Radhakrishnan H, Sakadžić S, Mandeville ET, Lo EH, Sosnovik DE, Srinivasan VJ (2012) Optical coherence tractography using intrinsic contrast. Opt Lett 37:3882–3884
Goh JO, Siong SC, Park D, Gutchess A, Hebrank A, Chee MW (2004) Cortical areas involved in object, background, and object-background processing revealed with functional magnetic resonance adaptation. J Neurosci 24(45):10223–10228. https://doi.org/10.1523/JNEUROSCI.3373-04.2004
Gong G, He Y, Concha L, Lebel C, Gross DW, Evans AC, Beaulieu C (2009) Mapping anatomical connectivity patterns of human cerebral cortex using in vivo diffusion tensor imaging tractography. Cereb Cortex 19(3):524–536. https://doi.org/10.1093/cercor/bhn102
Gungor A, Baydin S, Middlebrooks EH, Tanriover N, Isler C, Rhoton AL Jr (2017) The white matter tracts of the cerebrum in ventricular surgery and hydrocephalus. J Neurosurg 126(3):945–971. https://doi.org/10.3171/2016.1.JNS152082
Hagmann P, Kurant M, Gigandet X, Thiran P, Wedeen VJ, Meuli R, Thiran JP (2007) Mapping human whole-brain structural networks with diffusion MRI. PLoS One 2(7):e597. https://doi.org/10.1371/journal.pone.0000597
Hecaen H, Tzortzis C, Rondot P (1980) Loss of topographic memory with learning deficits. Cortex 16(4):525–542
Heiervang E, Behrens TEJ, Mackay CE, Robson MD, Johansen-Berg H (2006) Between session reproducibility and between subject variability of diffusion MR and tractography measures. Neuroimage 33:867–877
Henderson JM, Larson CL, Zhu DC (2008) Full scenes produce more activation than close-up scenes and scene-diagnostic objects in parahippocampal and retrosplenial cortex: an fMRI study. Brain Cogn 66(1):40–49. https://doi.org/10.1016/j.bandc.2007.05.001
Honey CJ, Kotter R, Breakspear M, Sporns O (2007) Network structure of cerebral cortex shapes functional connectivity on multiple time scales. Proc Natl Acad Sci USA 104(24):10240–10245. https://doi.org/10.1073/pnas.0701519104
Ino T, Inoue Y, Kage M, Hirose S, Kimura T, Fukuyama H (2002) Mental navigation in humans is processed in the anterior bank of the parieto-occipital sulcus. Neurosci Lett 322(3):182–186
Ino T, Doi T, Hirose S, Kimura T, Ito J, Fukuyama H (2007) Directional disorientation following left retrosplenial hemorrhage: a case report with fMRI studies. Cortex 43(2):248–254
Ito K, Sasaki M, Takahashi J, Uwano I, Yamashita F, Higuchi S, Goodwin J, Harada T, Kudo K, Terayama Y (2015) Detection of early changes in the parahippocampal and posterior cingulum bundles during mild cognitive impairment by using high-resolution multi-parametric diffusion tensor imaging. Psychiatry Res Neuroimaging 231(3):346–352
Janzen G, van Turennout M (2004) Selective neural representation of objects relevant for navigation. Nature Neurosci 7(6):673–677. https://doi.org/10.1038/nn1257
Johansen-Berg H, Behrens TE (2006) Just pretty pictures? What diffusion tractography can add in clinical neuroscience. Curr Opin Neurol 19(4):379–385. https://doi.org/10.1097/01.wco.0000236618.82086.01
Johansen-Berg H, Rushworth MF (2009) Using diffusion imaging to study human connectional anatomy. Annu Rev Neurosci 32:75–94. https://doi.org/10.1146/annurev.neuro.051508.135735
Jones DK, Cercignani M (2010) Twenty-five pitfalls in the analysis of diffusion MRI data. NMR Biomed 23:803–820
Jones DK, Christiansen KF, Chapman RJ, Aggleton JP (2013a) Distinct subdivisions of the cingulum bundle revealed by diffusion MRI fibre tracking: implications for neuropsychological investigations. Neuropsychologia 51(1):67–78
Jones DK, Knösche TR, Turner R (2013b) White matter integrity, fiber count, and other fallacies: the do's and don'ts of diffusion MRI. Neuroimage 73:239–254
Karavasilis E, Christidi F, Velonakis G, Giavri Z, Kelekis NL, Efstathopoulos EP, Evdokimidis I, Dellatolas G (2018) Ipsilateral and contralateral cerebro cerebellar white matter connections: a diffusion tensor imaging study in healthy adults. J Neuroradiol. https://doi.org/10.1016/j.neurad.2018.07.004
Katayama K, Takahashi N, Ogawara K, Hattori T (1999) Pure topographical disorientation due to right posterior cingulate lesion. Cortex 35(2):279–282
Keil B, Blau JN, Biber S, Hoecht P, Tountcheva V, Setsompop K, Triantafyllou C, Wald LL (2013) A 64-channel 3T array coil for accelerated brain. MRI Magn Reson Med 70:248–258
Kier EL, Staib LH, Davis LM, Bronen RA (2004a) MR imaging of the temporal stem: anatomic dissection tractography of the uncinate fasciculus, inferior occipitofrontal fasciculus, and Meyer's loop of the optic radiation. AJNR Am J Neuroradiol 25(5):677–691
Kier EL, Staib LH, Davis LM, Bronen RA (2004b) Anatomic dissection tractography: a new method for precise MR localization of white matter tracts. Am J Neuroradiol 25(5):670–676
King JA, Burgess N, Hartley T, Vargha-Khadem F, O'Keefe J (2002) Human hippocampus and viewpoint dependence in spatial memory. Hippocampus 12(6):811–820. https://doi.org/10.1002/hipo.10070
Klingler J (1935) Erleichterung der makrokopischen Präparation des Gehirns durch den Gefrierprozess. Orell Füssli, Zurich
Klingler J, Ludwig E (1956) Atlas Cerebri Humani. Karger, Basel
Knauff M, Kassubek J, Mulack T, Greenlee MW (2000) Cortical activation evoked by visual mental imagery as measured by fMRI. Neuroreport 11(18):3957–3962
Koutsarnakis C, Liakos F, Kalyvas AV, Sakas DE, Stranjalis G (2015) A laboratory manual for stepwise cerebral white matter fiber dissection. World Neurosurg 84(2):483–493. https://doi.org/10.1016/j.wneu.2015.04.018
Koutsarnakis C, Liakos F, Liouta E, Themistoklis K, Sakas D, Stranjalis G (2016) The cerebral isthmus: fiber tract anatomy, functional significance, and surgical considerations. J Neurosurg 124(2):450–462. https://doi.org/10.3171/2015.3.JNS142680
Koutsarnakis C, Liakos F, Kalyvas AV, Komaitis S, Stranjalis G (2017a) Letter to the Editor: White matter fiber tract architecture and ventricular surgery. J Neurosurg 126(4):1368–1371. https://doi.org/10.3171/2016.9.JNS162239
Koutsarnakis C, Liakos F, Kalyvas AV, Skandalakis GP, Komaitis S, Christidi F, Karavasilis E, Liouta E, Stranjalis G (2017b) The superior frontal transsulcal approach to the anterior ventricular system: exploring the sulcal and subcortical anatomy using anatomic dissections and diffusion tensor imaging tractography. World Neurosurg 106:339–354
Koutsarnakis C, Kalyvas AV, Komaitis S, Liakos F, Skandalakis GP, Anagnostopoulos C, Stranjalis G (2018) Defining the relationship of the optic radiation to the roof and floor of the ventricular atrium: a focused microanatomical study J Neurosurg:1–12 https://doi.org/10.3171/2017.10.JNS171836
Kravitz DJ, Saleem KS, Baker CI, Mishkin M (2011) A new neural framework for visuospatial processing. Nat Rev Neurosci 12(4):217–230. https://doi.org/10.1038/nrn3008
Le Bihan D, Poupon C, Amadon A, Lethimonnier F (2006) Artifacts and pitfalls in diffusion MRI. J Magn Reson Imaging JMRI 24(3):478–488. https://doi.org/10.1002/jmri.20683
Lee AC, Buckley MJ, Pegman SJ, Spiers H, Scahill VL, Gaffan D, Bussey TJ, Davies RR, Kapur N, Hodges JR, Graham KS (2005) Specialization in the medial temporal lobe for processing of objects and scenes. Hippocampus 15(6):782–797. https://doi.org/10.1002/hipo.20101

Magnain C et al (2014) Blockface histology with optical coherence tomography: a comparison with Nissl staining. Neuroimage 84:524–533. https://doi.org/10.1016/j.neuroimage.2013.08.072

Maguire EA, Frackowiak RS, Frith CD (1997) Recalling routes around london: activation of the right hippocampus in taxi drivers. J Neurosci 17(18):7103–7110

Malykhin N, Concha L, Seres P, Beaulieu C, Coupland NJ (2008) Diffusion tensor imaging tractography and reliability analysis for limbic and paralimbic white matter tracts. Psychiatry Res 164(2):132–142. https://doi.org/10.1016/j.pscychresns.2007.11.007

Mamata H, Mamata Y, Westin CF, Shenton ME, Kikinis R, Jolesz FA, Maier SE (2002) High-resolution line scan diffusion tensor MR imaging of white matter fiber tract anatomy. AJNR Am J Neuroradiol 23(1):67–75

Mandonnet E, Capelle L, Duffau H (2006) Extension of paralimbic low grade gliomas: toward an anatomical classification based on white matter invasion patterns. J Neuro-Oncol 78(2):179–185. https://doi.org/10.1007/s11060-005-9084-y

Martino J, Vergani F, Robles SG, Duffau H (2010) New insights into the anatomic dissection of the temporal stem with special emphasis on the inferior fronto-occipital fasciculus: implications in surgical approach to left mesiotemporal and temporoinsular structures. Neurosurgery 66(3 Suppl Operative):4–12. https://doi.org/10.1227/01.NEU.0000348564.28415.FA

Martino J, De Witt Hamer PC, Berger MS et al (2013) Analysis of the subcomponents and cortical terminations of the perisylvian superior longitudinal fasciculus: a fiber dissection and DTI tractography study. Brain Struct Funct 218:105–121

Mori S, Zhang J (2006) Principles of diffusion tensor imaging and its applications to basic neuroscience research. Neuron 51(5):527–539

Mori S, Crain BJ, Chacko VP, van Zijl PC (1999) Three-dimensional tracking of axonal projections in the brain by magnetic resonance imaging. Ann Neurol 45(2):265–269

Mori S, Wakana S, Van Zijl PC, Nagae-Poetscher L (2005) MRI atlas of human white matter. Elsevier, Oxford

Nimsky C, Bauer M, Carl B (2016) Merits and limits of tractography techniques for the uninitiated. In: Schramm J (ed) Advances and technical standards in neurosurgery. Advances and technical standards in neurosurgery, vol 43. Springer, Cham

O'Craven KM, Kanwisher N (2000) Mental imagery of faces and places activates corresponding stiimulus-specific brain regions. J Cogn Neurosci 12(6):1013–1023

Oouchi H, Yamada K, Sakai K, Kizu O, Kubota T, Ito H, Nishimura T (2007) Diffusion anisotropy measurement of brain white matter is affected by voxel size: underestimation occurs in areas with crossing fibers. AJNR Am J Neuroradiol 28(6):1102–1106. https://doi.org/10.3174/ajnr.A0488

Osawa A, Maeshima S, Kunishio K (2008) Topographic disorientation and amnesia due to cerebral hemorrhage in the left retrosplenial region. Eur Neurol 59(1–2):79–82. https://doi.org/10.1159/000109572

Pallis CA (1955) Impaired identification of faces and places with agnosia for colours; report of a case due to cerebral embolism. J Neurol Neurosurg Psychiatry 18(3):218–224

Palm C et al (2010) Towards ultra-high resolution fibre tract mapping of the human brain-registration of polarised light images and reorientation of fibre vectors. Front Hum Neurosci 4:9

Pascalau R, Stănilă RP, Sfrângeu S, Szabo B (2018) Anatomy of the limbic white matter tracts as revealed by fiber dissection and tractography. World Neurosurg 113:e672–e689. https://doi.org/10.1016/j.wneu.2018.02.121

Peltier J, Verclytte S, Delmaire C, Deramond H, Pruvo JP, Le Gars D, Godefroy O (2010a) Microsurgical anatomy of the ventral callosal radiations: new destination, correlations with diffusion tensor imaging fiber-tracking, and clinical relevance. J Neurosurg 112(3):512–519. https://doi.org/10.3171/2009.6.JNS081712

Peltier J, Verclytte S, Delmaire C, Pruvo JP, Godefroy O, Le Gars D (2010b) Microsurgical anatomy of the temporal stem: clinical relevance and correlations with diffusion tensor imaging fiber tracking. J Neurosurg 112(5):1033–1038. https://doi.org/10.3171/2009.6.JNS08132

Petrides M (2012) The human cerebral cortex: an MRI atlas of the sulci and gyri in MNI stereotaxic space. Elsevier/Academic Press, New York

Ploner CJ, Gaymard BM, Rivaud-Pechoux S, Baulac M, Clemenceau S, Samson S, Pierrot-Deseilligny C (2000) Lesions affecting the parahippocampal cortex yield spatial memory deficits in humans. Cereb Cortex 10(12):1211–1216

Powell HW, Guye M, Parker GJ, Symms MR, Boulby P, Koepp MJ, Barker GJ, Duncan JS (2004) Noninvasive in vivo demonstration of the connections of the human parahippocampal gyrus. Neuroimage 22(2):740–747. https://doi.org/10.1016/j.neuroimage.2004.01.011

Rosenbaum RS, Ziegler M, Winocur G, Grady CL, Moscovitch M (2004) "I have often walked down this street before": fMRI studies on the hippocampus and other structures during mental navigation of an old environment. Hippocampus 14(7):826–835. https://doi.org/10.1002/hipo.10218

Sachs H (1892) Das Hemisphärenmark des menschlichen Grosshirns: Der Hinterhauptlappen/von Heinrich Sachs. Thieme, Leipzig

Sarubbo S, Benedictis A, Maldonado IL et al (2013) Frontal terminations for the inferior fronto-occipital fascicle: anatomical dissection, DTI study and functional considerations on a multicomponent bundle. Brain Struct Funct 218:21–37

Schmahmann J, Pandya D (2009) Fiber pathways of the brain. OUP, Oxford

Setsompop K, Kimmlingen R, Eberlein E, Witzel T, Cohen-Adad J, McNab JA, Keil B, Tisdall MD, Hoecht P, Dietz P, Cauley SF, Tountcheva V, Matschl V, Lenz VH, Heberlein K, Potthast A, Thein H, Van Horn J, Toga A, Schmitt F, Lehne D, Rosen BR, Wedeen V, Wald LL (2013) Pushing the limits of in vivo diffusion MRI for the Human Connectome Project. Neuroimage 80:220–233

Seunarine KK, Alexander DC (2014) Multiple fibers: beyond the diffusion tensor. In: Johansen-Berg H, Behrens TE (eds) Diffusion MRI, 2nd edn. Elsevier, New York, USA, pp 105–123

Shrout PE, Fleiss JL (1979) Intraclass correlations: uses in assessing rater reliability. Psychol Bull 86(2):420–428

Silva SM, Andrade JP (2016) Neuroanatomy: the added value of the Klingler method. Ann Anat 208:187–193

Spiers HJ, Maguire EA (2006) Thoughts, behaviour, and brain dynamics during navigation in the real world. Neuroimage 31(4):1826–1840. https://doi.org/10.1016/j.neuroimage.2006.01.037

Spiers HJ, Maguire EA (2007) The neuroscience of remote spatial memory: a tale of two cities. Neuroscience 149(1):7–27. https://doi.org/10.1016/j.neuroscience.2007.06.056

Sugiura M, Shah NJ, Zilles K, Fink GR (2005) Cortical representations of personally familiar objects and places: functional organization of the human posterior cingulate cortex. J Cogn Neurosci 17(2):183–198. https://doi.org/10.1162/0898929053124956

Takahashi N, Kawamura M, Shiota J, Kasahata N, Hirayama K (1997) Pure topographic disorientation due to right retrosplenial lesion. Neurology 49(2):464–469

Takao H, Hayashi N, Kabasawa H, Ohtomo K (2012) Effect of scanner in longitudinal diffusion tensor imaging studies. Hum Brain Mapp 33:466–477

Thiebaut de Schotten M, Urbanski M, Valabregue R, Bayle DJ, Volle E (2014) Subdivision of the occipital lobes: an anatomical and functional MRI connectivity study. Cortex 56:121–137. https://doi.org/10.1016/j.cortex.2012.12.007

Thomas C, Ye FQ, Irfanoglu MO et al (2014) Anatomical accuracy of brain connections derived from diffusion MRI tractography is inherently limited. Proc Natl Acad Sci 111:16574–16579

Tournier J, Calamante F, Connelly A (2012) MRtrix: diffusion tractography in crossing fiber regions. Int J Imaging Syst Technol 22(1):53–66

Ture U, Yasargil MG, Friedman AH, Al-Mefty O (2000) Fiber dissection technique: lateral aspect of the brain. Neurosurgery 47(2):417–426 **(discussion 417–426)**

Vann SD, Aggleton JP, Maguire EA (2009) What does the retrosplenial cortex do? Nat Rev Neurosci 10(11):792–802. https://doi.org/10.1038/nrn2733

Veenith TV et al (2013) Inter subject variability and reproducibility of diffusion tensor imaging within and between different imaging sessions. PLoS One 8:e65941. https://doi.org/10.1371/journal.pone.0065941

Vergani F, Mahmood S, Morris CM, Mitchell P, Forkel SJ (2014) Intralobar fibres of the occipital lobe: a post mortem dissection study. Cortex 56:145–156. https://doi.org/10.1016/j.cortex.2014.03.002

Vos SB, Jones DK, Viergever MA, Leemans A (2011) Partial volume effect as a hidden covariate in DTI analyses. Neuroimage 55(4):1566–1576. https://doi.org/10.1016/j.neuroimage.2011.01.048

Wakana S, Caprihan A, Panzenboeck MM, Fallon JH, Perry M, Gollub RL, Hua K, Zhang J, Jiang H, Dubey P, Blitz A, van Zijl P, Mori S (2007) Reproducibility of quantitative tractography methods applied to cerebral white matter. Neuroimage 36(3):630–644. https://doi.org/10.1016/j.neuroimage.2007.02.049

Wang H et al (2011) Reconstructing micrometer-scale fiber pathways in the brain: multi-contrast optical coherence tomography based tractography. Neuroimage 58:984–992

Whittingstall K, Bernier M, Houde JC, Fortin D, Descoteaux M (2014) Structural network underlying visuospatial imagery in humans. Cortex 56:85–98. https://doi.org/10.1016/j.cortex.2013.02.004

Wolbers T, Buchel C (2005) Dissociable retrosplenial and hippocampal contributions to successful formation of survey representations. J Neurosci 25(13):3333–3340. https://doi.org/10.1523/JNEUROSCI.4705-04.2005

Wu Y, Sun D, Wang Y, Wang Y, Ou S (2016) Segmentation of the cingulum bundle in the human brain: a new perspective based on DSI tractography and fiber dissection study. Front Neuroanat 10:84

Zemmoura I, Blanchard E, Raynal PI, Rousselot-Denis C, Destrieux C, Velut S (2016) How Klingler's dissection permits exploration of brain structural connectivity? An electron microscopy study of human white matter. Brain Struct Funct 221(5):2477–2486